

Computational Targeting Of RhoH Gtpase: An In Silico Drug Discovery Strategy Against Cancer Progression

N Sravanthi¹, U S H Raghavendra Prasad², N Ravi³, *M Kavitha³

Department of Chemistry, University College of Science, Osmania University, Hyderabad-500007, Telangana, India.

ABSTRACT

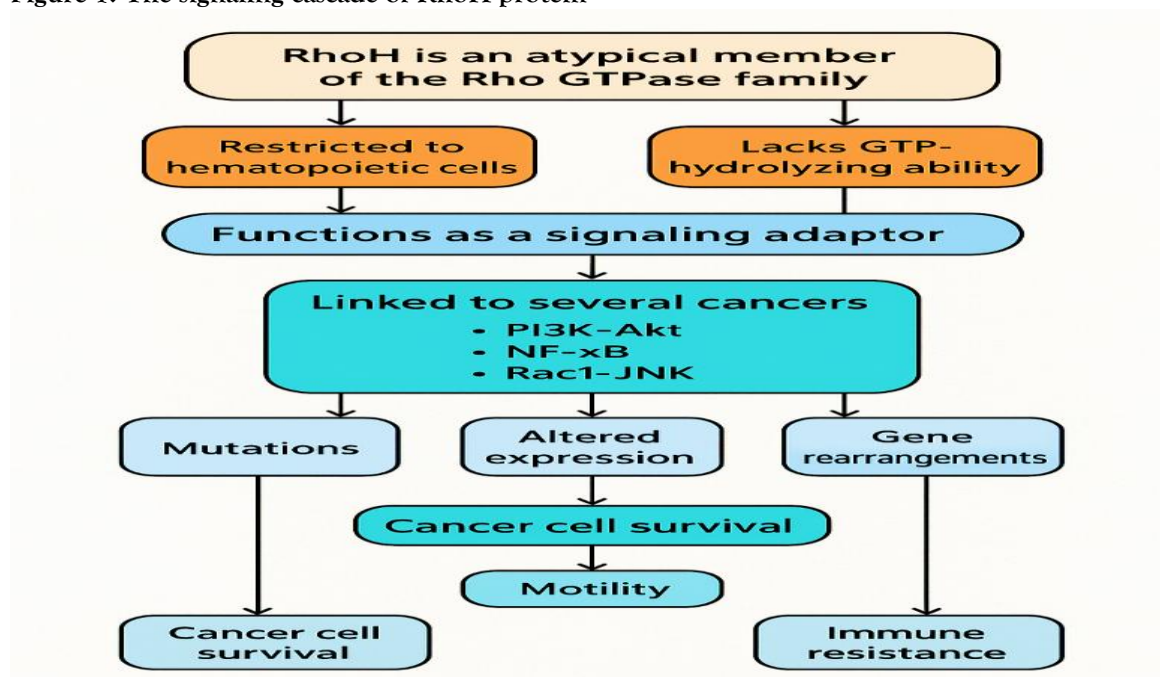
RhoH is an atypical Rho GTPase with restricted expression in hematopoietic cells and lacks intrinsic GTPase activity [1]. Although it regulates T-cell receptor signaling [2], recent studies link RhoH to tumour-related mechanisms such as immune evasion [3], enhanced survival [4], and metastasis [5] through P13K-Akt [6], NF- κ B [7], and Rac1-JNK pathways [8]. To explore its therapeutic potential, we constructed a 3D homology model of RhoH and validated it structurally. Docking simulations revealed interactions with Rac1, ZAP-70 [9], and drug-like ligands, identifying key binding residues. This study provides new structural insights into RhoH and supports its role as a candidate for targeted cancer therapy development.

Keywords: Rho GTPase, P13K-Akt [6], NF- κ B [7], and Rac1-JNK pathway

INTRODUCTION

Cancer encompasses a wide range of disorders marked by uncontrolled cell growth, evasion of programmed cell death, persistent blood vessel formation, and the capacity to invade nearby tissues and spread to distant sites. These malignant traits are often driven by abnormal activation of cellular signalling pathways that reshape the tumour environment. Among the molecular players influencing these events are Rho GTPases, which regulate processes like cell movement, growth, and immune responses. RhoH is an atypical member of this family, restricted to hematopoietic cells and lacking the GTP-hydrolysing ability seen in other Rho proteins. Rather than acting as a switch, RhoH functions as a signalling adaptor. It was initially recognized for its role in T-cell activation but is now linked to several cancers through mutations, altered expression, or gene rearrangements. By affecting pathways such as P13K-Akt, NF- κ B, and Rac1-JNK [10], RhoH contributes to cancer cell survival, mobility, and immune resistance, making it promising target for structural and therapeutic research.

Figure 1. The signaling cascade of RhoH protein



2. METHODOLOGY

In recent times, computational chemistry has emerged as a powerful tool to address the challenges associated with conventional drug discovery techniques. Despite ongoing efforts, the complete three-dimensional (3D) structure of the RhoH protein remains unresolved through both laboratory experiments and in silico modeling. Consequently, this section focuses on constructing and validating a 3D model of RhoH using computational strategies. The amino acid sequence of RhoH, provided in FASTA format, was obtained from the UniProt database ^[11]. To find appropriate structural templates, proteins exhibiting similar domain architecture, folding patterns, and secondary structures were identified with the aid of prediction tools like BLAST ^[12], PHYRE2 ^[13]. Sequence-to-structure alignments were further assessed using the E-value, a metric that reflects the degree of similarity between RhoH and the selected templates.

Protein sequence Alignment and 3D model construction

The amino acid sequence of the target protein was aligned with template sequences using CLUSTALW ^[14]. A 3D structural model of RhoH was then constructed using MODELLER ^[15], which employs the CHARMM22 force field to guide the modeling process. From the multiple models produced, the one exhibiting the lowest objective function value was chosen for subsequent refinement and optimization.

Energy minimization and Validation

To improve the precision of the predicted 3D structure, loop regions were refined and energy minimization was carried out using the Impref module within the Schrodinger software suite, employing a 0.3 Å cut-off. This step utilized the OPLS2004 (Optimized Potentials for Liquid Simulations) force field ^[16] to preserve the native geometry of the protein's carbon backbone. Throughout the minimization process, the backbone atoms were restrained, allowing only the side chains to adjust their positions. This approach enabled the model to reach stable, low-energy conformation without altering the coordinates of the α atoms. To enhance the structural stability of the model, molecular dynamics simulations were performed using the Protein Preparation Wizard integrated in the Schrodinger Suite ^[16]. During this procedure, the OPLS-AA (all-atom) force field was applied to further refine and optimize the 3D conformation of the protein. The quality and credibility of the homology models were assessed using validation tools including PROCHECK ^[17], ProSA ^[18]. To measure the structural similarity between RhoH and its chosen template, root mean square deviation (RMSD) analysis was conducted. The conformation exhibiting the highest structural stability was selected for in-depth analysis, with particular attention given to its secondary structure elements and potential active site regions.

Active site identification by computational approach

Accurately determining a protein's active site is crucial for elucidating its biological role and plays a fundamental part in structure-based drug discovery. Computational approaches are often employed to predict potential ligand-binding regions within the protein's three-dimensional structure. Tools such as CASTp ^[19] and SiteMap ^[20], available in the Schrodinger suite, are widely utilized to identify hydrophobic cavities and geometrically favorable areas for ligand interaction.

Virtual Screening and Molecular Docking

To facilitate molecular docking and virtual screening, a receptor grid was generated at the predicted binding site of the RhoH protein using the Glide module within the Schrodinger software suite. Ligand structures were obtained from established molecular databases and prepared using LigPrep, which optimizes features such as stereochemistry, ionization states, and ring conformations to enhance docking reliability. The virtual screening workflow was conducted in sequential phases, utilizing Glide's HTVS (High Throughput Virtual Screening), SP (Standard Precision), and XP (Extra Precision) modes. After docking, the ligands were assessed and ranked based on their Glide Scores, reflecting their estimated binding affinities.

a) ADMET Properties

Comprehensive evaluation of Absorption, Distribution, Metabolism, Excretion, and Toxicity (ADMET) ^[21] properties is essential during the initial phases of drug development, as these parameters heavily influence clinical trial outcomes and a drug candidate's commercial viability. Ligands that demonstrated

high binding affinity to RhoH during virtual screening and docking were further analysed for their pharmacokinetic behaviour using the QikProp module in the Schrodinger suite.

3. RESULTS AND DISCUSSION

Modeling and Structural evaluation of the RhoH protein

a) Template selection using amino acid sequence of RhoH protein

The UniProt database is a cornerstone in bioinformatics, offering a meticulously curated repository of protein sequences and their corresponding annotations, which supports a broad array of biological research applications. By consolidating data from renowned sources such as Swiss-Prot, TrEMBL, and PIR, UniProt delivers detailed insights into protein sequences, their functional annotations, structural properties, and taxonomic classifications. Its user-friendly interface simplifies protein searches, utilizing query-based tools that allow the efficient retrieval and downloading of FASTA-formatted sequences, which are vital for high-level bioinformatics investigations. In this study, the UniProt platform was employed to retrieve the protein sequences of RhoH protein, which were then subjected to analysis for obtaining functional annotations and exploring structural features. These sequences were instrumental in identifying conserve domains and active sites, essential for homology modelling endeavours. By utilizing protein accession numbers or sequence-specific queries, UniProt provided and reproducible data, playing a crucial role in the computational workflow. The BLAST (Basic Local Alignment Search Tool) server was used to identify an appropriate structural template for RhoH protein, a critical protein involved in regulate cytoskeleton dynamics, cell morphology and polarity, cell motility, vesicle trafficking, cell survival, differentiation and new gene expression, cell cycle progression and cell growth. The FASTA sequence of RhoH protein was submitted to the Protein Data Bank (PDB) using the BLASTP algorithm. The selection process emphasized template with high sequence identity, low E-values (<0.001), and substantial query coverage to ensure precise structural modeling and biological relevance. Among the options, a template 1KI1_A with 42.25% sequence identity, an E-value of $3 \times e^{-52}$, and 94% query coverage was chosen for its strong similarity to RhoH Protein. This selected template served as a reliable starting point for 3D structural modeling and analysis, underlining the value BLAST server in homology-based protein structure predictions. Similarly, the PHYRE2 server identifies template proteins with comparable fold architectures. It provides a confidence score to indicate the likelihood of sequence similarity between the target amino acid sequence and the template structures. This similarity is further evaluated using statistical metrics such as E-values and percentage confidence. Based on these analyses, a template 1KI1_A is selected for constructing the three-dimensional structure of the RhoH protein (Table 3.1)

Table 3.1. Selection of template for The RhoH protein

S. NO.	Server tool	Identified Template	E -Value/ Confidence score	Identity %
1	BLAST	1KI1_A	$3 \times e^{-52}$	94
3	Phyre2	1KI1_A	99.6%	95

b) Comparative Sequence Analysis and Structural Characterization of the RhoH protein

The RhoH protein sequence was aligned with selected template 1KI1_A, using the CLUSTALW tool for sequence alignment (Figure 4.1)

Figure 3.1. Sequence alignment of the RhoH protein with the template 1KI1_A

```

sp|Q15669|RHOH  M L S S I K C V L V G D S A V G K T S L L V R F T S E T F P E A Y K P T V Y E N T G V D V
1KI1_1|Chains    - M Q T I K C V V G D G A V G K T C L L I S Y T T N K F P S E Y V P T V F D N Y A V T V
Alignment_Conse M X X X I K C V X V G D X A V G K T X L L X X X T X X X F P X X Y X P T V X X N X X V X V
sp|Q15669|RHOH  F M D G I Q I S L G L W D T A G N D A F R S I R P L S Y Q Q A D V V L M C Y S V A N H N S
1KI1_1|Chains    M I G G E P Y T L G L F D T A G Q E D Y D R L R P L S Y P Q T D V F L V C F S V V S P S S
Alignment_Conse X X X G X X X X L G L X D T A G X X X X X R P L S Y X Q X D V X L X C X S V X X X X S
sp|Q15669|RHOH  F L N L K N K W I G E I R S N L P C T P V L V V A T Q T D Q R E - - - - - M G P H R A
1KI1_1|Chains    F E N V K E K W V P E I T H C P K T P F L L V G T Q I D L R D D P S T I E K L A K N K Q
Alignment_Conse F X N X K X K W X X E I X X X X P X T P X L X V X T Q X D X R X D P S T I E K X X X X X X
sp|Q15669|RHOH  S C V N A M E G K K L A Q D V R A K G Y L E C S A L S N R G V Q Q V F E C A V R T A V N Q
1KI1_1|Chains    K P I T P E T A E K L A R D L K A V K Y V E C S A L T Q K G L K N V F D E A I L A A L E P
Alignment_Conse X X X X X X X X K L A X D X X A X X Y X E C S A L X X X G X X V F X X A X X A X X X X
sp|Q15669|RHOH  A R R R N R R R L F S I N E C K I F
1KI1_1|Chains    P E P K K S R R S - - - - -
Alignment_Conse X X X X X R R X F S I N E C K I F

```

Figure 3.1. Illustrated the sequence alignment of the RhoH protein with its corresponding template 1KI1_A sequence. The alignment was performed using CLUSTALW and subsequently visualized through Discovery Studio in the figure, identical amino acids are shown with dark blue color, strong similarity are shown in blue color, weak similarity are shown in light blue color and non-matching are shown in white color. The FASTA sequence of the RhoH protein, along with the chosen template sequence and their corresponding atomic coordinates, was submitted to the MODELLER software to construct a three dimensional model of RhoH protein. A total 100 initial models were generated, and the one with the lowest Modeller objective function score was selected for subsequent optimization analysis.

4. VALIDATION OF MODEL GENERATED BY COMPUTATIONAL METHOD

The stereochemical integrity of the RhoH protein structure was evaluated using a Ramachandran plot analysis (Figure 4.1)

Figure 4.1. Ramachandran contour plot of the protein RhoH (Stereochemical Integrity)

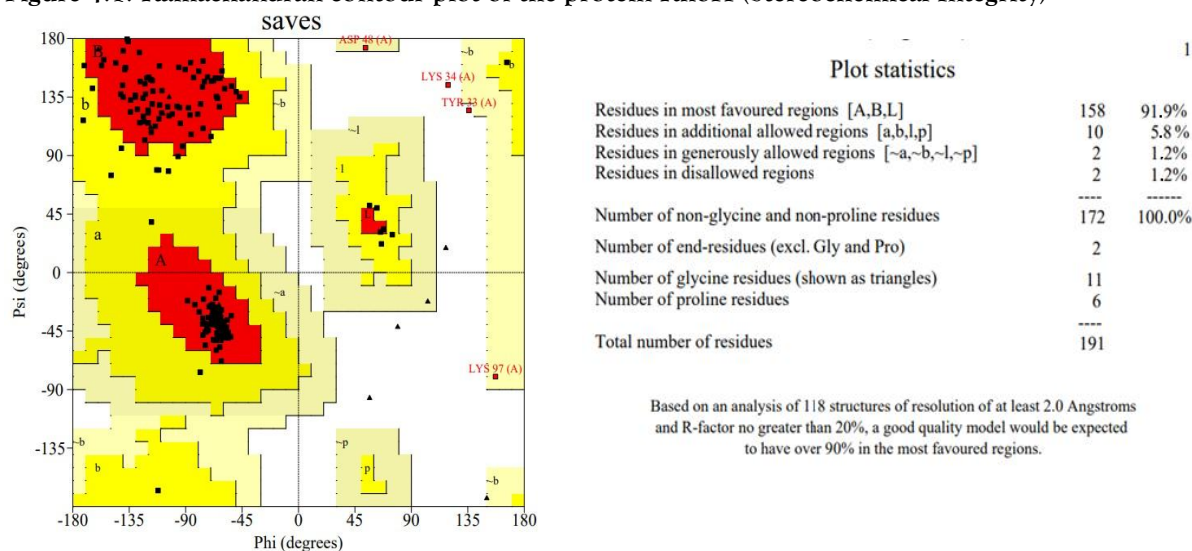
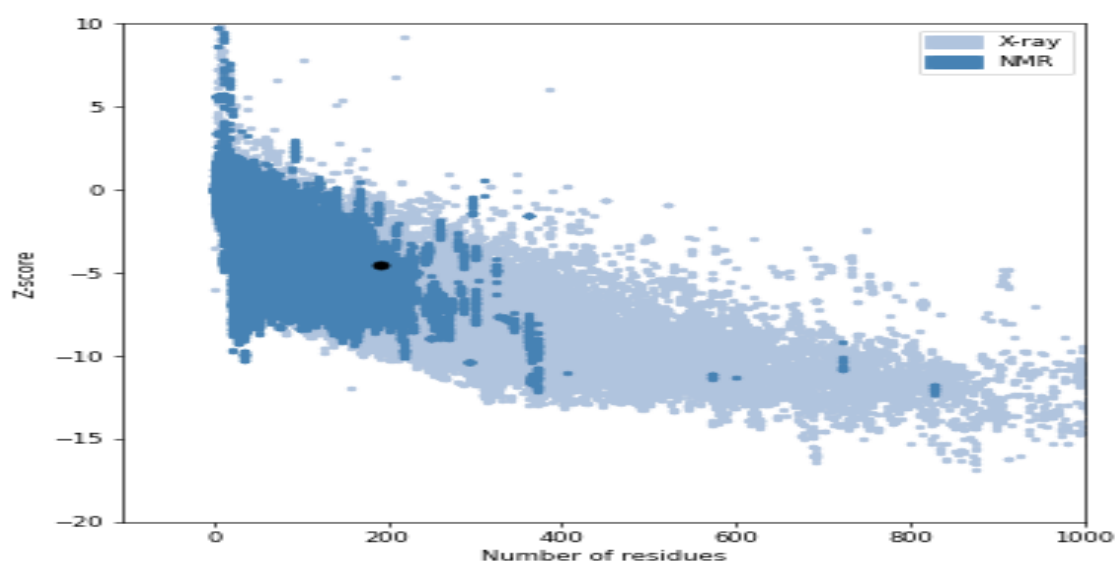


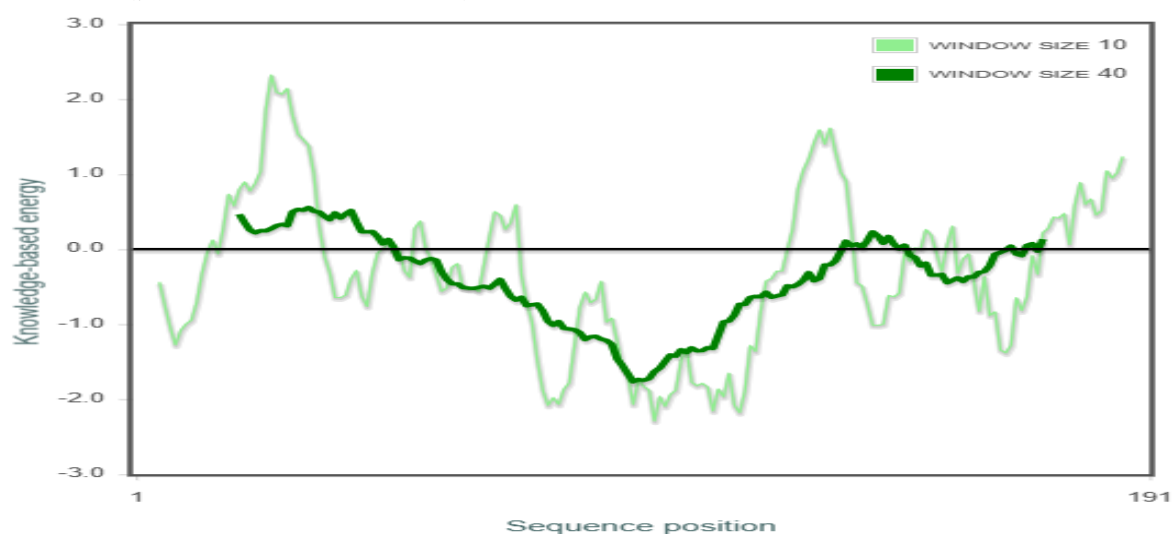
Figure 4.1 displays the Ramachandran plot^{[22] [23]} for the RhoH protein structure, illustrating the distribution of residues (Shown as black dots) across various energetically favorable region. These regions are color-coded, with red denoting the most favorable zones, yellow representing additionally allowed areas, and light yellow indicating generously allowed regions. The analysis confirms that all residues of the RhoH protein fall within these energetically permissible zones.

Figure 4.2. ProSA Server predicted Z-Score of the RhoH protein



In addition, the overall structural integrity of the RhoH protein model was examined using the ProSA (Protein Structure Analysis) server ^[24]. The resulting Z-score of -4.56 (Figure 4.2) falls within the typical range observed for experimentally determined protein structures of similar size, whether resolved through X-ray crystallography (light blue) or NMR spectroscopy (dark blue), suggesting a reliable model. ProSA energy profile ^[25] (Figure 4.3) presents the calculated energy values for the structure across two segment lengths-windows of 10 and 40 amino acids-offering into localized energy variations within the model.

Figure 4.3. RhoH protein Local Model Quality



5. Secondary Structure Profile

Figure 5.1. The 3D structure of the RhoH protein

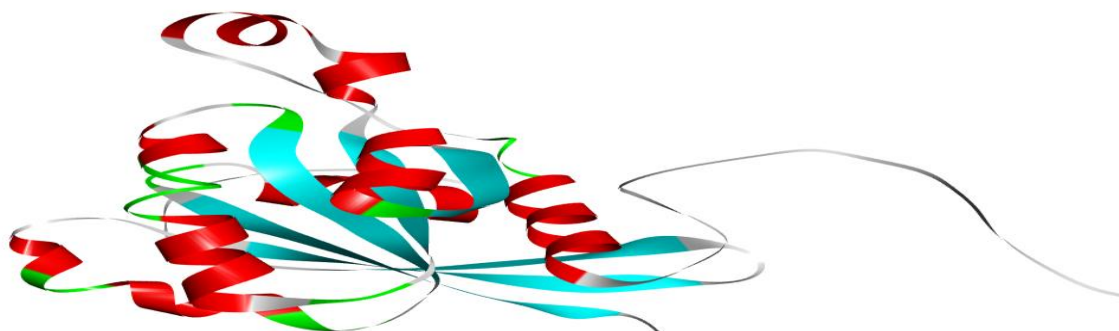
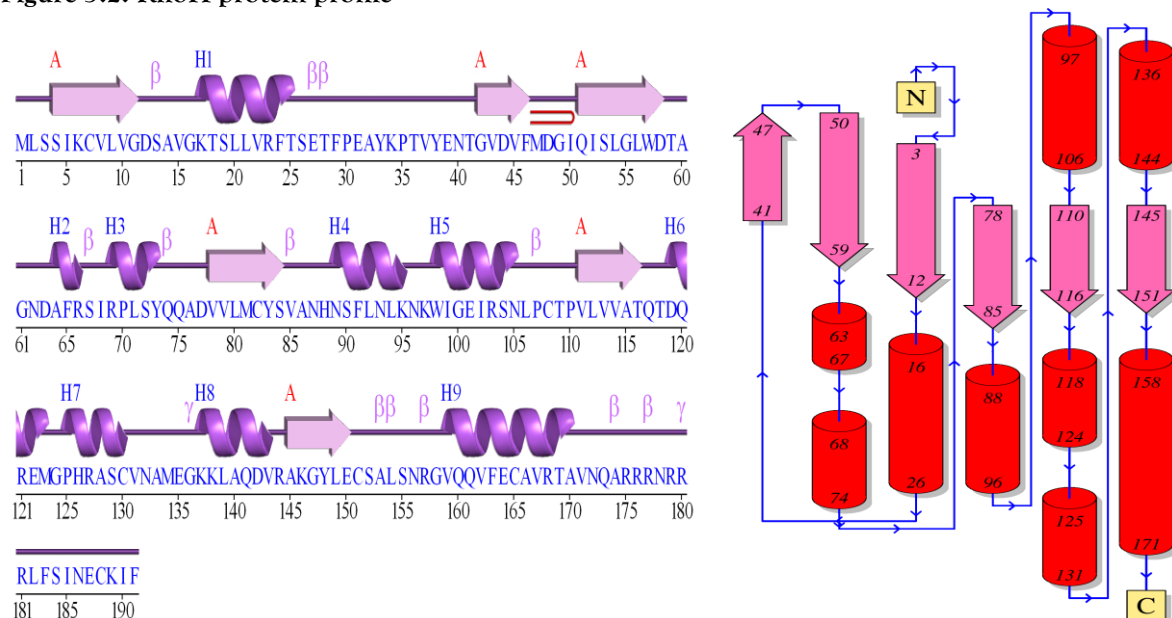


Figure illustrates the three-dimensional structure of the RhoH protein, presented as a cartoon diagram. In this representation, the N-terminal is positioned at the top right, while the C-terminal is located at the bottom right. The three dimensional structure of the RhoJ protein comprises 9 α helices and 6 β sheets (Figure 5.1 and Table 5.1)

Figure 5.2. RhoH protein profile



After submission of the generated 3D- model with PDB ID **lib7** is analyzed and shown in Figure 5.2 presents the secondary structural features of the RhoH protein as generated by the PDB-sum server tool [26]. In this visualization, 9 α -helices are depicted in dark violet, 6 β -sheets are represented by pink arrows and as well as in cylindrical form of RhoH, α helices (red color), β sheets (pink arrows) are represented.

Table 5.1. The α -helices and β -sheets in RhoH protein

S. NO.	Type of secondary structure	Amino acid sequences From to To
1	α helices	16 to 26 63 to 67 68 to 74 88 to 96 97 to 106 118 to 124 125 to 131 136 to 144 158 to 171
2	β sheets	3 to 12 41 to 47 50 to 59 78 to 85 110 to 116 145 to 151

Table lists the α - helices and β – sheets identified within the RhoH protein structure, a total of 9 α helices, 6 β – sheets.

6. Identification of Putative active sites

In silico analyses were performed using advanced structural bioinformatics tools, namely CASTp and SiteMap, to predict potential ligand-binding regions within the protein. The CASTp server evaluates

topographical features of protein surfaces by applying both Connolly's molecular surface model and Richards' solvent – accessible surface model to identify and characterize putative binding pockets. Complementary predictions generated by SiteMap revealed a high probability active sites.

Table 6.1. RhoH protein active site regions

S. NO.	Active site prediction server / tool	Site Number	Volume (Å)	Amino acids
1	SiteMap	1	235.641	5,47,48,50,52,112, 137,140,141,144, 145,146,147,148, 149,164,165,167, 168,170,171,176, 177,178
2	CASTp	1	443.862	47,48,167,168, 171,172,173,174, 175,177,181,183, 184,186,188

Table 6.1 indicating one active site region identified using SiteMap and CASTp server tools. The putative active sites shown by SiteMap starting from 5 to 178 with a volume of 235.641Å and CASTp showing an active site starting from 47 to 188 with a volume of 443.862 Å.

7. Screening of Ligand Molecules and Docking Studies

In this research, a structure-based virtual screening (SBVS) strategy was applied to discover new small molecules that can interact with the RhoH protein. The docking simulations were guided by a receptor grid centered on the RhoH active site, with grid dimensions set to 23 Å × 27.56 Å × 1.33 Å. Ligand preparation was carried out using the LigPrep module from the Schrödinger software suite, which generated low-energy conformers for each compound. The Epik tool, integrated within LigProp (Schrödinger Suite) ^[27], was used to predict multiple ionization and tautomeric states based on Hammett and Taft parameters, allowing for the generation of up to eight tautomeric variants per molecule by default. To ensure chemical and stereochemical validity, the software automatically corrected structural irregularities, such as incorrect ring geometries or chirality issues often encountered in natural product scaffolds. A total of 30,000 compounds sourced from the Comprehensive Marine Natural Products Database (CMNPD) ^{[28] [29] [30]} were processed, yielding 44,850 unique ligand structures. These were then evaluated using a tiered virtual screening approach via Glide (Schrödinger, LLC, New York, NY, 2023), which included High Throughput Virtual Screening (HTVS), followed by Standard Precision (SP), and finally Extra Precision (XP) docking stages. At each level roughly the top 10% of compounds—those showing the most promising binding poses—were advanced to the next phase in accordance with Glide's default filtering mechanisms. The screening process ultimately identified five high-scoring ligand-RhoH complexes. These top candidates, selected based on their docking scores, are summarized in Figure 7.1 and Table 7.1. Similar SBVS frameworks have been previously utilized in the literature for lead compound discovery targeting novel therapeutic proteins. An in-depth examination of the docking outcomes demonstrated strong ligand-protein interactions, suggesting high binding affinities between the compounds and the RhoH protein. Visualization of hydrogen bond interactions was carried out using Schrodinger suite ^{[31][32]}, with bond lengths ranging from 1.61 Å to 2.78 Å, which fall within a meaningful and favorable range (refer Table 8.1). The 3D and corresponding 2D interaction profiles for the selected ligand-RhoH complexes (D1 to D5) are depicted in Figure 7.1.

Figure 7.1. Ligands (D1 to D5) – RhoH Protein interactions

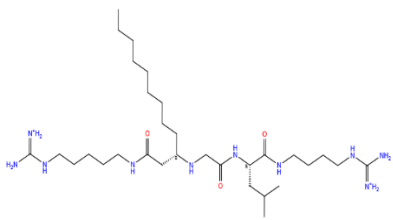
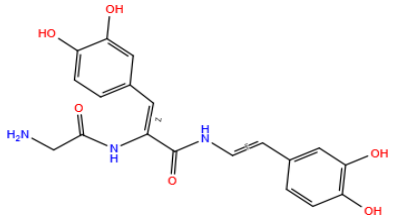
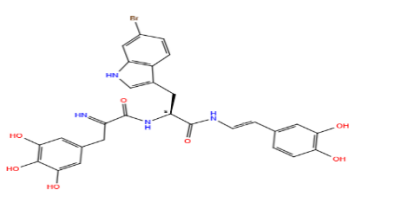
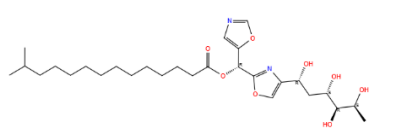
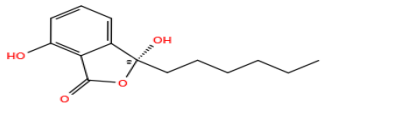
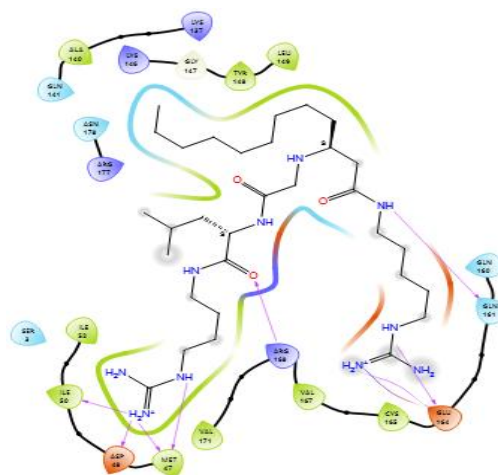
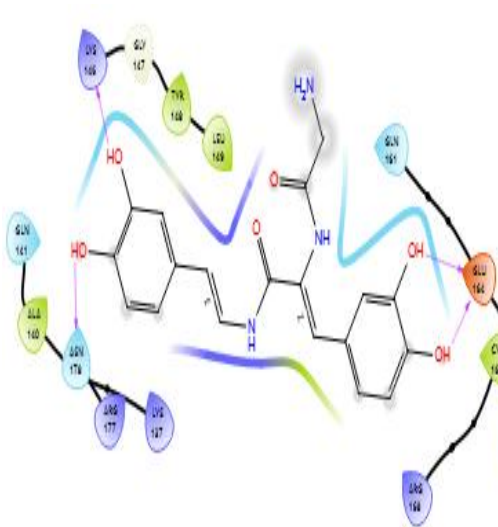
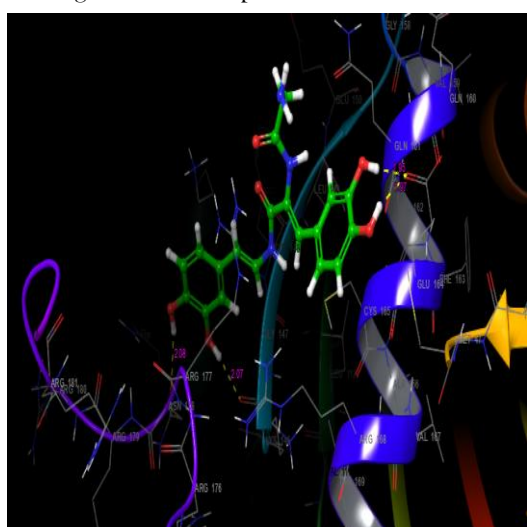
S. NO.	Ligand	Glide Score	Glide Energy (Kcal/mol)	Hydrogen bond between ligand and amino acid	Hydrogen Bond Distance
D1		-7.005	-56.922	D1-ARG168 D1-GLN161 D1-MET47 D1-ASP48 D1-GLU164 D1-GLU164 D1-ILE50 D1-MET47	2.53 2.02 2.00 2.23 1.61 1.88 2.28 1.91
D2		-7.042	-53.027	D2-GLU164 D2-GLU164 D2-ASN178 D2- ALA146	1.95 1.97 2.08 2.07
D3		-7.498	-51.102	D3-MET47 D3-MET47(A) D3-ARG177 D3-ARG177 D3-TYR148 D3-TYR148 D3-GLN161 D3-GLU164(A)	1.98 2.63 2.38 2.32 1.89 1.94 2.08 2.38
D4		-6.206	-50.631	D4-GLN161 D4-ARG168 D4-GLU164	1.93 2.12 1.92
D5		-7.006	-60.867	D5-LYS137 D5-TYR148 D5-LYS146(A)	2.34 1.89 2.78

Figure 7.1. Ligand – RhoH protein docked complexes

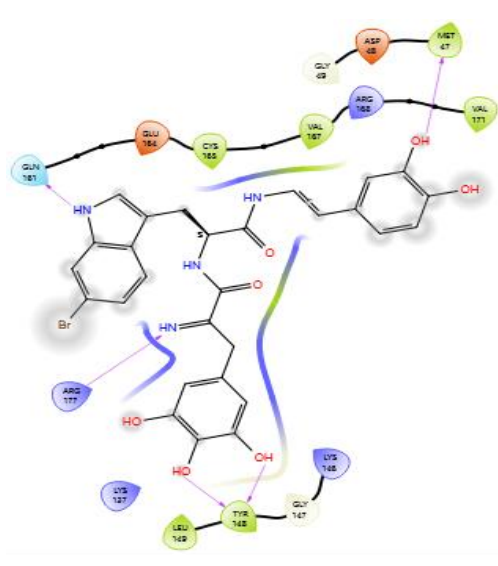
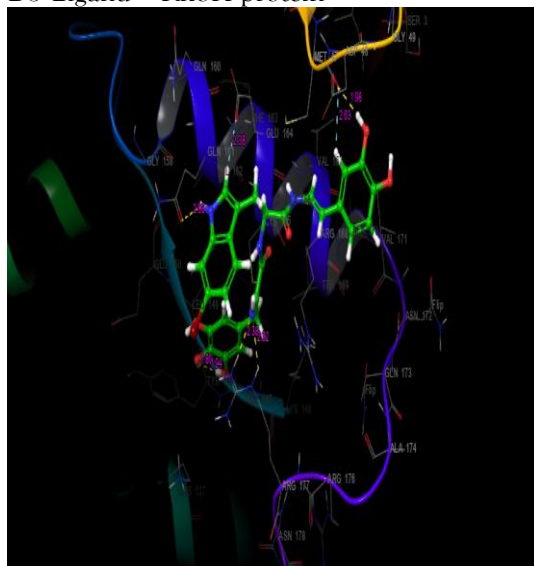
D1 Ligand - RhoH protein



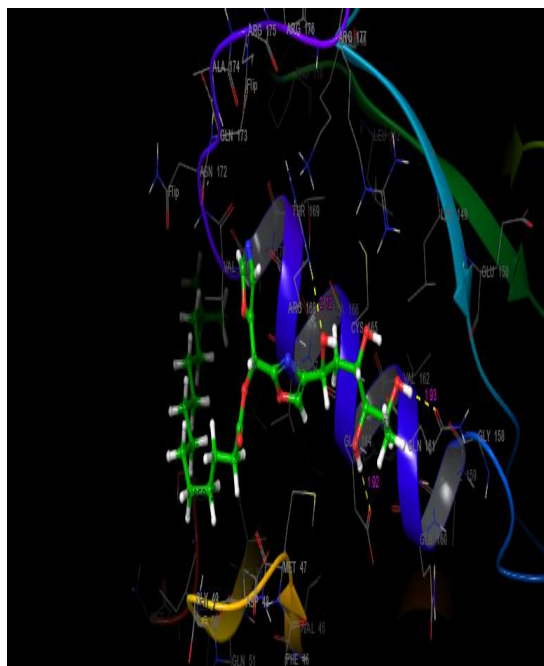
D2 Ligand - RhoH protein



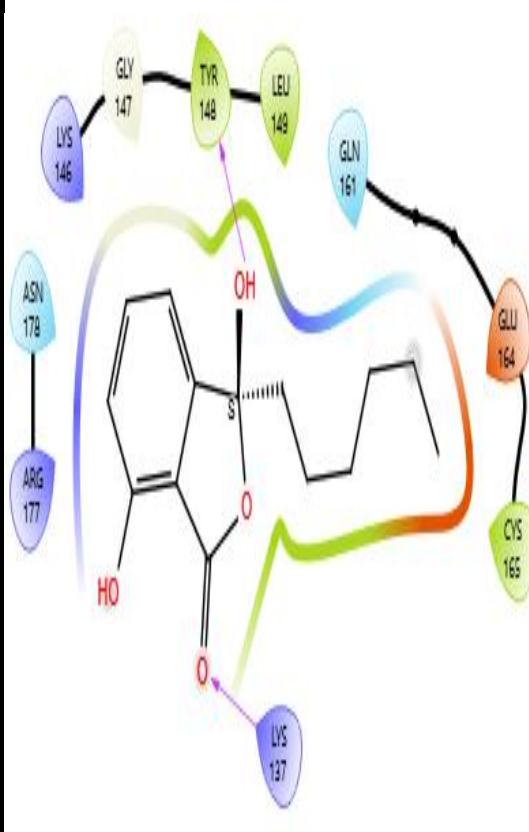
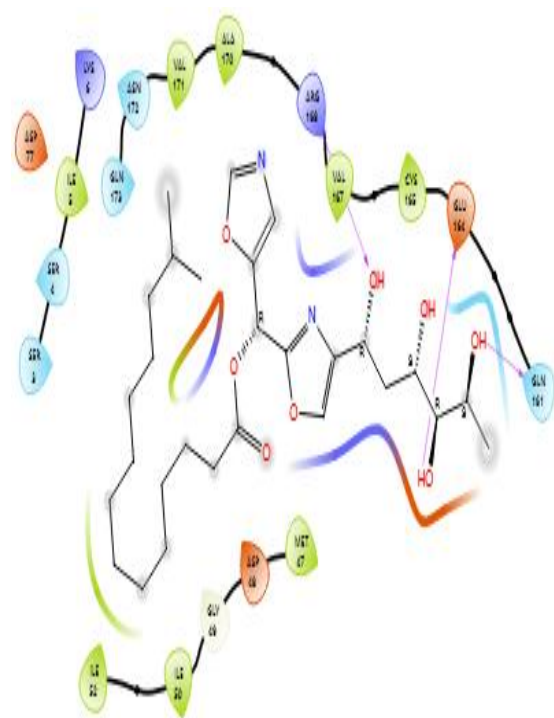
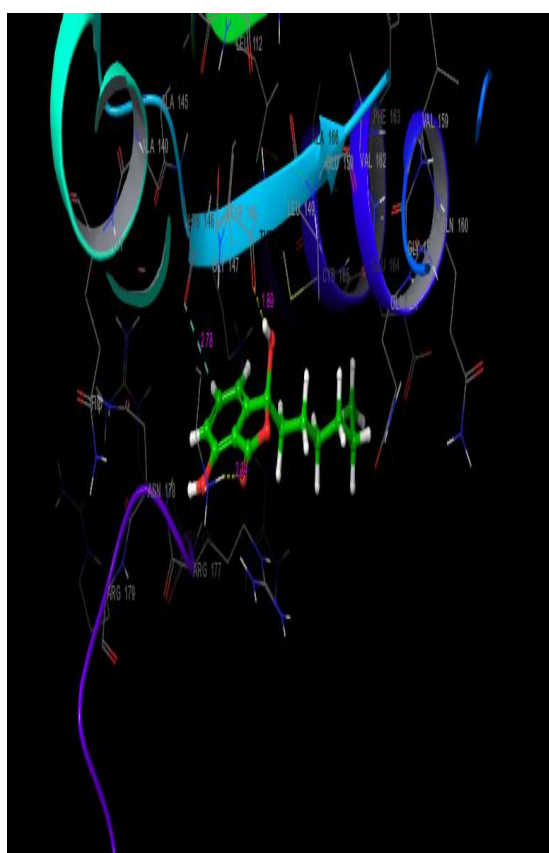
D3 Ligand - RhoH protein



D4 Ligand – RhoH protein



D5 Ligand – RhoH protein



8. ADMET properties

Figure 8.1. Recommended ADME profile

S. No.	Descriptor	ADME property	permissible ranges or recommended value
1	CNS	Predicted central nervous system activity on -2 to +2 scale	-2 (inactive) to +2 (active)
2	mol_MW	Molecular weight of the molecule	130 to 725
3	DHB	Estimated number of hydrogen bonds that would be donated by the solute to water molecules in an aqueous solution	0 to 6
4	AHB	Estimated number of hydrogen bonds that would be accepted by the solute from water molecules in an aqueous solution	2 to 20
5	QPPCaco	Predicted apparent Caco-2 cell permeability in nm/sec	<25 poor, >500 great
6	QPlogPw	Predicted water/gas partition coefficient.	4.0 – 45.0
7	QPlogPo/w	Predicted octanol/water partition coefficient	-2.0 – 6.5
8	QPlogS	Predicted aqueous solubility, log S, S in mol dm ⁻³	-6.5 – 0.5
9	QPlogKhsa	Prediction of binding to human serum albumin	-1.5 – 1.5
10	QPlogHERG	Predicted IC ₅₀ value for blockage of HERG K ⁺ channels	Below +5.0
11	QPlogBB	Predicted blood / partition coefficient	-3.0 – 1.2
12	% human oral absorption	Predicted human oral absorption on 0 to 100% scale	>80% is high <25% is poor
13	Rule Of Five	Number of violations of Lipinski's rule of five	maximum is 4
14	Rule Of Three	Number of violations of Jorgensen's rule of three	maximum is 3
15	Synthetic feasibility	Predicted synthetic feasibility: on scale of 1 to 10;	0 = high feasibility 10 = least feasible
16	Lipophilicity	Predicted lyophilic nature of the ligand calculated from pIC50-LogP	min -6; max +3

a) Physicochemical Profile

Preclinical assessment plays a crucial role in the early stages of drug development. In this investigation, ADME (Absorption, Distribution, Metabolism, and Excretion) analysis^{[33] [34] [35]} was performed on the newly identified ligands using the QikProp module integrated within the Schrödinger suite (figure). The evaluated physicochemical properties-including molecular weight (≤ 624.912 Da), number of hydrogen bond donors (≤ 5.25), and hydrogen bond acceptors (≤ 12.8) -were all within the generally accepted thresholds for drug-like compounds, as illustrated in Figure 8.1.

b) Pharmacokinetic Properties

Human Oral Absorption (HOA) is a crucial and essential pharmacokinetic parameter during the initial phases of drug development. In this study, all candidate ligands exhibited strong HOA values, ranging from 69.233 to 100%, suggesting excellent potential for oral bioavailability (Table 8.1). As shown in Figure 8.1, all compounds evaluated met the standard criteria for effective oral absorption (refer Table 8.1).

Aqueous solubility, a critical factor influencing both absorption and systemic distribution, was evaluated using the QPlogS descriptor. The calculated solubility values for the compounds spanned from -6.315 to -1.97, which are within acceptable ranges for drug-like molecules. To estimate intestinal permeability, the QPPCaco descriptor was used; it yielded values between 675.07 and 521.665, indicating the compounds have sufficient permeability to cross the gastrointestinal barrier (refer Table 8.1). Additionally, the extent of protein binding-particularly to human serum albumin-was assessed through QPlogKhsa values. These values, which reflect serum protein affinity, ranged from -0.783 to -0.081, suggesting that all ligands fall within the pharmacologically acceptable range for plasma interaction (refer Table 8.1)

Table 8.1 The ADME profile of ligands D1 to D5 obtained from virtual screening

Ligand Number	Physicochemical Properties				Pharmacokinetic Properties							Drug Likeness Property		
	mol_MW	donorHB	acptHB	QPlogS	HOA%	QPPCaco	QPlogKhsa	QPlogPw	QPlogBB	CNS	QPlogHERG	RuleOfFive	RuleOfThree	QPlogPo/w
D1	624.912	5.25	11.25	-3.353	100	600.145	-0.783	29.827	-2.254	-2	-3.127	3	1	1.442
D2	385.376	4.25	8.25	-1.97	76.351	521.665	-0.597	21.583	-2.301	-2	-3.896	1	2	-0.273
D3	609.432	3.25	9	-5.446	85.67	675.07	0.026	24.138	-2.075	-2	-4.893	3	2	2.559
D4	538.68	4	12.8	-6.315	69.233	672.509	-0.081	17.947	-2.951	-2	-1.094	1	2	3.749
D5	250.294	3	10	-4.521	75.25	563.21	-0.152	18.256	-2.635	-2	-1.022	1	1	2.546

Considering the potential risks associated with unintended blood-brain barrier (BBB) permeability and its impact on the central nervous system (CNS), QPlogBB values were examined. The results indicated that all compounds fell within an acceptable range of -2.951 to -2.075 (Table 8.1), suggesting minimal ability to penetrate the CNS. Additionally, all ligands exhibited negative CNS activity scores, implying low neurotoxicity potential and favorable CNS safety profiles. Furthermore, inhibition of the hERG (human ether-a-go-go-related gene) potassium channel is a well-established concern in cardiac safety, as it can lead to QT interval prolongation and increase the risk of arrhythmias. To assess this, predicted pIC50 values for hERG channel inhibition were calculated and found to range from -4.893 to -1.022. These values indicate a low likelihood of cardio toxic effects among the tested ligands.

Toxicity Summary

To assess the metabolic vulnerabilities of the compounds, their potential interactions with Cytochrome P450 enzymes were evaluated using The ProTox 3.0 platform^{[36][37][38]} (Table 8.2). The analysis revealed that several ligands either inhibited or did not affect major CYP450 isoform-an important factor in predicting metabolic stability and possible drug-drug interactions. Additionally, the compounds demonstrated no sign of hepatotoxicity or cardiotoxicity. Collectively, these findings suggest that the selected molecules possess favorable pharmacological properties and low toxicity profiles, highlighting their promise as therapeutic candidates for treating cancer.

Table 8.2 The Toxic profiling of the ligands D1 to D5 using ProTox server

S. NO.	LIGANDS	HEPATOTOXICITY	CARDIOTOXICITY	CYP-1A2	CYP-2C19	CYP-2C9	CYP-2D6	CYP-3A4
1	D1	INACTIVE	INACTIVE	INACTIVE	INACTIVE	INACTIVE	INACTIVE	INACTIVE
2	D2	INACTIVE	INACTIVE	INACTIVE	INACTIVE	INACTIVE	INACTIVE	INACTIVE
3	D3	INACTIVE	INACTIVE	INACTIVE	INACTIVE	INACTIVE	INACTIVE	ACTIVE
4	D4	INACTIVE	INACTIVE	INACTIVE	INACTIVE	ACTIVE	INACTIVE	INACTIVE
5	D5	INACTIVE	INACTIVE	INACTIVE	INACTIVE	INACTIVE	INACTIVE	INACTIVE

CONCLUSION

The computational inhibition of RhoH-an atypical Rho GTPase implicated in hematopoietic malignancies-represents a promising therapeutic strategy. This study highlights the potential of in silico

drug discovery approaches to identify small-molecule inhibitors capable of targeting aberrant RhoH activity resulting from mutations, dysregulated expression, or chromosomal arrangements. By disrupting RhoH-mediated signalling cascades, including PI3K – Akt, NF- κ B, and Rac1-JNK pathways, such interventions may suppress cancer cell survival, motility, and immune evasion. These findings underscore the value of structure-based virtual screening and ADMET profiling in the early identification of candidate compounds for modulating oncogenic adaptors like RhoH, thereby advancing targeted cancer therapy development.

Acknowledgement

Authors are thankful to Osmania University for providing computational software's.

REFERENCES

- Vega, F. M., & Ridley, A. J. (2008). Rho GTPases in cancer cell biology. *FEBS Letters*. Link
- Ahmad Mokhtar, A. M., et al. (2021). The role of RhoH in TCR signalling and its involvement in diseases. *Cells*, 10(4), 950. PDF
- Haga, R. B., & Ridley, A. J. (2016). Rho GTPases: Regulation and roles in cancer cell biology. *Small GTPases*, 7(4), 207–221. PDF
- Ahmad Mokhtar, A. M., Hashim, I. F., & Makhtar, M. M. Z. (2021). The role of RhoH in TCR signalling and its involvement in diseases. *Cells*, 10(4), 950. <https://www.mdpi.com/2073-4409/10/4/950>
- Allen, R., Tajadura-Ortega, V., Garg, R., Owczarek, C., Bright, M. D., & Ridley, A. J. (2018). An RNAi screen of Rho signalling networks identifies RhoH as a regulator of Rac1 in prostate cancer cell migration. *BMC Biology*, 16(1), 1–18. <https://link.springer.com/article/10.1186/s12915-018-0489-4>
- Ridley, A. J. (2004). Rho proteins and cancer. *Breast Cancer Research and Treatment*, 84(1), 13–19. <https://link.springer.com/article/10.1023/B:BREA.0000018423.47497.c6>
- Haga, R. B., & Ridley, A. J. (2016). Rho GTPases: Regulation and roles in cancer cell biology. *Small GTPases*, 7(4), 207–221. <https://www.tandfonline.com/doi/abs/10.1080/21541248.2016.1232583>
- Aspenström, P. (2022). The role of fast-cycling atypical RHO GTPases in cancer. *Cancers*, 14(8), 1961. <https://www.mdpi.com/2072-6694/14/8/1961>
- Kuang, M., Zhou, Z., Lu, Z., Shen, W., Ge, H., et al. (2023). Prognostic prediction of lung adenocarcinoma by integrative analysis of RHOH expression and methylation. *The Clinical Respiratory Journal*. <https://onlinelibrary.wiley.com/doi/abs/10.1111/crj.13574>
- Ridley, A. J., & Collard, J. G. (2003). Role of Rho-family proteins in cell adhesion and cancer. *Current Opinion in Cell Biology*, 15(5), 583–590. <https://www.sciencedirect.com/science/article/pii/S095506740300098X>
- The UniProt Consortium. (2023). UniProt: the Universal Protein Knowledgebase in 2023. *Nucleic Acids Research*, 51(D1), D523–D531. <https://doi.org/10.1093/nar/gkac1052>
- Camacho, C., Coulouris, G., Avagyan, V., Ma, N., Papadopoulos, J., Bealer, K., & Madden, T. L. (2009). BLAST+: architecture and applications. *BMC Bioinformatics*, 10, 421. <https://doi.org/10.1186/1471-2105-10-421>
- Kelley, L. A., et al. (2015). The Phyre2 web portal for protein modeling. *Nature Protocols*, 10(6), 845–858. <https://doi.org/10.1038/nprot.2015.053>
- Thompson, J. D., et al. (1994). CLUSTAL W: improving the sensitivity of progressive multiple sequence alignment. *Nucleic Acids Res*, 22(22), 4673–4680.
- Webb, B., & Sali, A. (2016). Comparative protein structure modeling using MODELLER. *Current Protocols in Bioinformatics*, 54(1), 5.6.1–5.6.37. <https://doi.org/10.1002/cpbi.3>
- Friesner, R. A., Banks, J. L., Murphy, R. B., Halgren, T. A., et al. (2004). Glide: A new approach for rapid, accurate docking and scoring. 1. Method and assessment of docking accuracy. *Journal of Medicinal Chemistry*, 47(7), 1739–1749. <https://doi.org/10.1021/jm0306430>
- Laskowski, R. A., MacArthur, M. W., Moss, D. S., & Thornton, J. M. (1993). PROCHECK: A program to check the stereochemical quality of protein structures. *Journal of Applied Crystallography*, 26(2), 283–291. <https://doi.org/10.1107/S0021889892009944>
- Wiederstein M & Sippl MJ (2007) ProSA-web: interactive web service for the recognition of errors in three-dimensional structures of proteins. *Nucleic Acids Res* 35, W407–W410
- Tian, W., et al. (2018). CASTp 3.0: computed atlas of surface topography of proteins. *Nucleic Acids Res*, 46(W1), W363–W367. <https://doi.org/10.1093/nar/gky473>
- Ibrahim, Z. Y., Abdulfatai, U., Ejeh, S., Ajala, A., & Adawara, S. N. (2024). QSAR and ADMET screening to assess antimalarial potential of Amodiaquine derivatives. *The Microbe*.
- R Dumpati, V Ramatenki, R Vadija, S Vellanki, U Vuruputuri. Structural insights into suppressor of cytokine signaling 1 protein-identification of new leads for type 2 diabetes mellitus, *Journal of Molecular Recognition* 31 (7), e2706

22. R Dumpati, R Dulapalli, B Kondagari, V Ramatenki, S Vellanki, R Vadija. Suppressor of cytokine signalling-3 as a drug target for type 2 diabetes mellitus: a structure-guided approach, *ChemistrySelect* 1 (10), 2502-2514
23. Ramachandran, G. N., Ramakrishnan, C., & Sasisekharan, V. (1963). Stereochemistry of polypeptide chain configurations. *Journal of Molecular Biology*, 7(1), 95-99. [https://doi.org/10.1016/S0022-2836\(63\)80023-6](https://doi.org/10.1016/S0022-2836(63)80023-6)
24. Wiederstein, M., & Sippl, M. J. (2007). ProSA-web: interactive web service for the recognition of errors in three-dimensional structures of proteins. *Nucleic Acids Research*, 35(suppl_2), W407-W410.
25. Prajapat, R., Marwal, A., & Gaur, R. K. (2014). Recognition of Errors in the Refinement and Validation of Three-Dimensional Structures of AC1 Proteins of Begomovirus Strains by Using ProSA-Web. *Journal of Viruses*, 2014, Article ID 752656. <https://doi.org/10.1155/2014/752656>
26. Laskowski, R. A. (2009). Protein structure databases. In O. Carugo & F. Eisenhaber (Eds.), *Data Mining Techniques for the Life Sciences* (pp. 55-79). Humana Press. https://doi.org/10.1007/978-1-60327-241-4_4
27. Sastry, G. M., Adzhigirey, M., Day, T., Annabhimoju, R., & Sherman, W. (2013). Protein and ligand preparation: Parameters, protocols, and influence on virtual screening enrichments. *Journal of Computer-Aided Molecular Design*, 27(3), 221-234.
28. Lyu, C., Chen, T., Qiang, B., Liu, N., Wang, H., et al. (2021). CMNPD: a comprehensive marine natural products database towards facilitating drug discovery from the ocean.
29. Afendi, F. M., Okada, T., Yamazaki, M., Hirai-Morita, A., Nakamura, Y., Nakamura, K., ... & Saito, K. (2020). CMNPD: A comprehensive marine natural products database towards facilitating drug discovery from the ocean. *Nucleic Acids Research*, 48(D1), D509-D516. <https://doi.org/10.1093/nar/gkz890>
30. Bhat, B. A., Algaissi, A., Khamjan, N. A., Dar, T. U. H., & Qasir, N. (2024). Exploration of CMNPD against Dengue viral NS1 protein using high-throughput computational studies. *Journal of Biomolecular Structure and Dynamics*. <https://doi.org/10.1080/07391102.2023.2297006>
31. Rocca, R., Alcaro, S., & Artese, A. (2024). Structure-based virtual screening and molecular dynamics simulations of FDA-approved drugs targeting MALAT1.
32. Chikhale, H. U., & Rishipathak, D. D. (2025). In silico prediction, molecular docking study for identification of novel nitrogen-substituted benzoxazole derivative for their potential biological activity.
33. Hasan et al. (2022) In silico molecular docking and ADME/T analysis of Quercetin compound with its evaluation of broad-spectrum therapeutic potential against particular human diseases *Informatics in Medicine Unlocked*, 29, 100911. Elsevier. <https://doi.org/10.1016/j.imu.2022.100911>
34. Verma et al. (2019) Pharmacophore modeling, 3D-QSAR, docking and ADME prediction of quinazoline based EGFR inhibitors *Arabian Journal of Chemistry*, 12(8), 2125-2137. Elsevier. <https://doi.org/10.1016/j.arabjc.2015.11.014>
35. Kumar et al. (2019) E-pharmacophore modelling, virtual screening, molecular dynamics simulations and in-silico ADME analysis for identification of potential E6 inhibitors against cervical cancer *Journal of Molecular Structure*, 1195, 203-213. <https://doi.org/10.1016/j.molstruc.2019.04.023>
36. Banerjee, P., et al. (2018). ProTox-II: prediction of toxicity of chemicals. *Nucleic Acids Res*, 46(W1), W257-W263. <https://doi.org/10.1093/nar/gky318>
37. Drwal, M. N., Banerjee, P., Dunkel, M., Wettig, M. R., & Preissner, R. (2014). ProTox: a web server for the in silico prediction of rodent oral toxicity. *Nucleic Acids Research*, 42(W1), W53-W58.
38. The prediction of acute toxicity (LD50) for organophosphorus-based chemical warfare agents (V-series) using toxicology in silico methods *Archives of Toxicology*, 98, 895-911. Springer. <https://doi.org/10.1007/s00204-023-03632-y>